Journal of Applied Mechanics and Technical Physics, Vol. 50, No. 3, pp. 447–453, 2009

FLOW STRUCTURE FORMED BY INTERACTION OF A SINGLE MICROJET WITH A SUPERSONIC JET FLOW

V. I. Zapryagaev and N. P. Kiselev

UDC 533.6.011.5

The flow structure at the initial section of a supersonic underexpanded jet in the presence of a stationary artificial disturbance in the form of a single microjet is studied experimentally. The influence of gas-dynamic and geometric parameters of the microjet on the structure of the main supersonic flow and a significant effect of the microjet on the changes in the Pitot pressure in the shear layer of the supersonic jets are identified. Interaction between the microjet and the main jet flow generates disturbances of two types propagating in the main jet flow: a disturbance induced by the wake flow behind the microjet and a weaker disturbance in the form of a low-intensity shock wave (Mach wave type).

Key words: *supersonic jet, micronozzle, microjet.*

The search for possibilities of mixing intensification in high-velocity flows is one of the basic problems of aerogasdynamics. It was found experimentally that the initial section of a supersonic non-isobaric jet exhausting from an axisymmetric nozzle has a three-dimensional structure in the shear layer.

Current research involves intensification of mixing processes by means of generation of streamwise vortex structures in supersonic jets of various configurations with the help of various vortex generators: corrugated surfaces, chevrons, tabs, lobed mixers. Collin et al. [1] changed the pressure in the microjet and studied the degree of its penetration into the main jet. The shear layer was shifted toward the jet axis thereby, and the magnitude of this shift depended on the pressure in the microjet. Microjet injection at an angle intensified the gas mixing processes. Alkislar et al. [2] studied the effect of injection of jets into the main flow formed by twin jets on the level of noise of the resultant flow. Two coaxial supersonic jets generated strong self-sustained pressure oscillations. The amplitude of the resultant high-frequency noise with screech tone reached high values. Injection of 16 microjets into the main supersonic flow at the exit of the micronozzles and the main nozzle (Mach number M = 1.5) led to significant reduction of the overall level of wide-band noise and to elimination of high-frequency noise at frequencies of 6 and 12 kHz. Jets injected into the main flow were used to suppress acoustic waves in the case of flow interaction with a plane obstacle in experiments simulating vertical takeoff and landing [3]. There are some papers that describe investigations of methods of decreasing the level of noise generated by the jet in supersonic jets by using nozzles with chevrons and tabs (see, e.g., [4]). Methods and devices that form streamwise vortices are intensely used now to intensify mixing and reduce the level of noise generated by the jet. Methods of controlling the mixing processes with the use of streamwise vortices generated by artificial disturbances in the form of microjets were described in [1–4].

The objective of the present activities is an experimental study of the flow structure at the initial section of a supersonic jet under the action of a single microjet on the main flow and the effect on microjet intensity and location of the interaction region on the interaction process.

The experiments were performed with cold air in a jet module of a T-326 hypersonic blowdown wind tunnel of the Khristianovich Institute of Theoretical and Applied Mechanics of the Siberian Division of the Russian Academy

Khristianovich Institute of Theoretical and Applied Mechanics, Siberian Division, Russian Academy of Sciences, Novosibirsk 630090; nkiselev@itam.nsc.ru. Translated from Prikladnaya Mekhanika i Tekhnicheskaya Fizika, Vol. 50, No. 3, pp. 104–111, May–June, 2009. Original article submitted April 25, 2008.

0021-8944/09/5003-0447

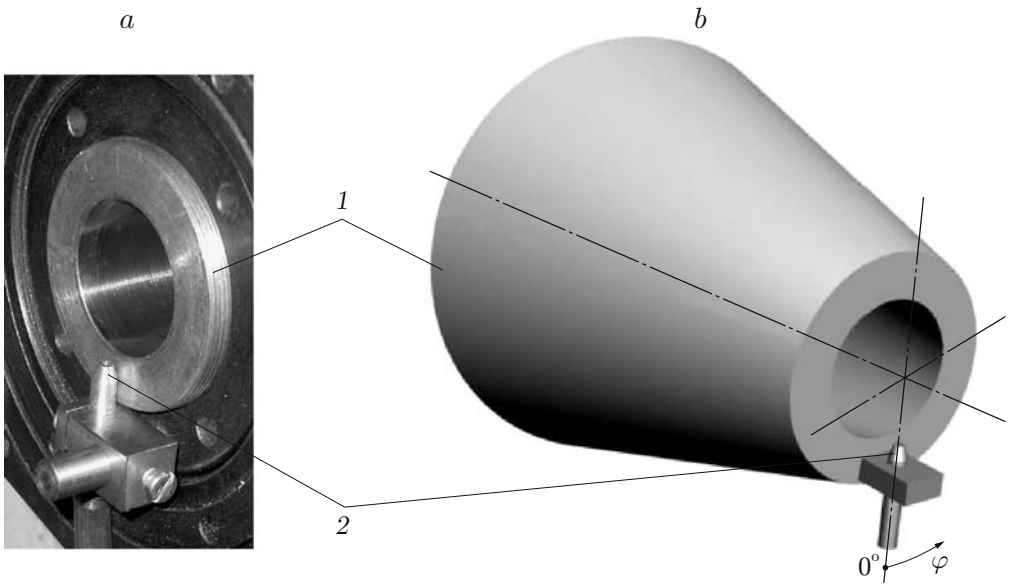

Fig. 1. Photograph (a) and sketch (b) of the main nozzle ($M_a = 1.0$) and the micronozzle device: 1) nozzle; 2) micronozzle.

of Sciences [5]. The microjet exhausted from a convergent nozzle (micronozzle) with an outer diameter $d = 3$ mm and an exit diameter $d_j = 1.5$ mm. The inner contour of the micronozzle was shaped as a cone (convergent micronozzle). The microjet was injected in the normal direction to the boundary of a supersonic underexpanded jet. The photograph and sketch of the main contoured nozzle and the microjet device are shown in Fig. 1. The shape of the inner radius of the main convergent nozzle corresponded to the Vitoshinskii profile, and its exit radius was $R_a = 15$ mm. The level of roughness of the inner surface of the main nozzle was determined as the mean height of microroughness elements on the nozzle contour, which was equal to $k \approx 0.25$ μm in our experiments. Exhaustion of a supersonic weakly underexpanded jet from the main nozzle with a Mach number $M_a = 1$ was organized. The pressure ratio of this jet was $n_p = P_a/P_c = 2.64$ (P_a is the pressure at the nozzle exit and P_c is the pressure in the test chamber of the jet module). The Reynolds number was calculated on the basis of the flow parameters and nozzle-exit diameter and equaled $\mathrm{Re}_d = 2.21 \cdot 10^6$. The gas-dynamic parameters of the microjet were varied by changing the pressure applied to the micronozzle P_{0j}, which took the values $P_{0j} = 0.12$, 0.20, and 0.41 MPa. At these values of the pressure P_{0j}, microjets with $N_j = P_{0j}/P_c = 1.33$, 2.22, and 4.44 were injected in the experiments. At $N_j = 1.33$, a high-velocity subsonic microjet was formed. At $N_j = 2.22$ and 4.44, exhaustion of supersonic microjets with a Mach number at the micronozzle exit $M_a = 1.0$ and pressure ratios $n_{pj} = 1.17$ (for $P_{0j} = 0.20$ MPa) and $n_{pj} = 2.35$ (for $P_{0j} = 0.41$ MPa) was observed. The microjet location characterized by the streamwise x_j and radial r_j coordinates of the micronozzle exit was also varied in the experiments. At a fixed value of P_{0j}, the Pitot pressure $P_t(x, r, \varphi)$ was measured by a Pitot tube in jet cross sections x as a function of the radial r and angular φ coordinates.

The schlieren photographs of the main underexpanded jet ($n_p = 2.64$) in the presence of a supersonic microjet ($N_j = 4.44$, $M_a = 1.0$, and $\mathrm{Re}_d = 0.4 \cdot 10^5$) and a supersonic weakly underexpanded microjet ($N_j = 4.44$) are shown in Fig. 2. The main supersonic flow is directed from left to right, and the microjet flow is directed from top to bottom. The flow pattern was visualized by the schlieren technique in an IAB-451 shadowgraph. The pictures were taken by a CV-M10 digital camera (resolution 640×480 pixels) produced by the JAI company. It is seen in Fig. 2 that the flow resulting from interaction of a supersonic underexpanded jet with a supersonic microjet has a shock-wave structure. Two symmetric waves directed along the flow and corresponding to the shock wave ahead of the microjet are clearly visible in the region of interaction of the microjet with the main flow. As the flow in the microjet is weakly underexpanded, a multibarrel flow structure is registered, which arises at moderate values of the pressure ratio in the non-interacting microjet (Fig. 2b). The flow structure in the microjet is similar to the flow structure in the main underexpanded jet. Figure 2b shows the microjet exhausting from the micronozzle whose

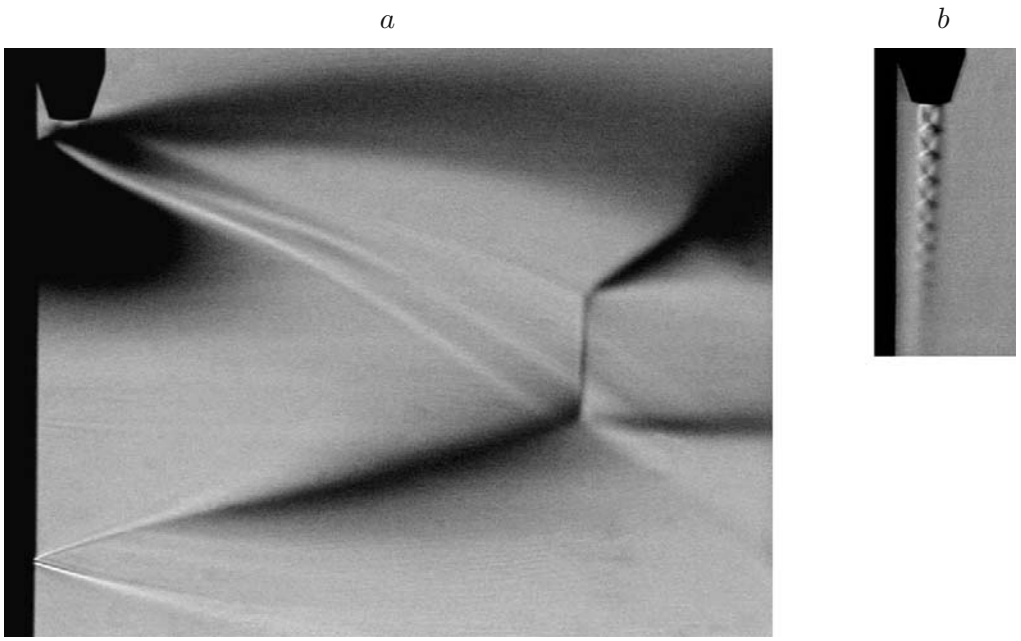

Fig. 2. Schlieren photographs of the main underexpanded jet ($M_a = 1.0$ and $n_p = 2.64$) in the presence of a supersonic microjet ($M_a = 1.0$ and $N_j = 4.44$) (a) and a supersonic weakly underexpanded microjet ($N_j = 4.44$) (b).

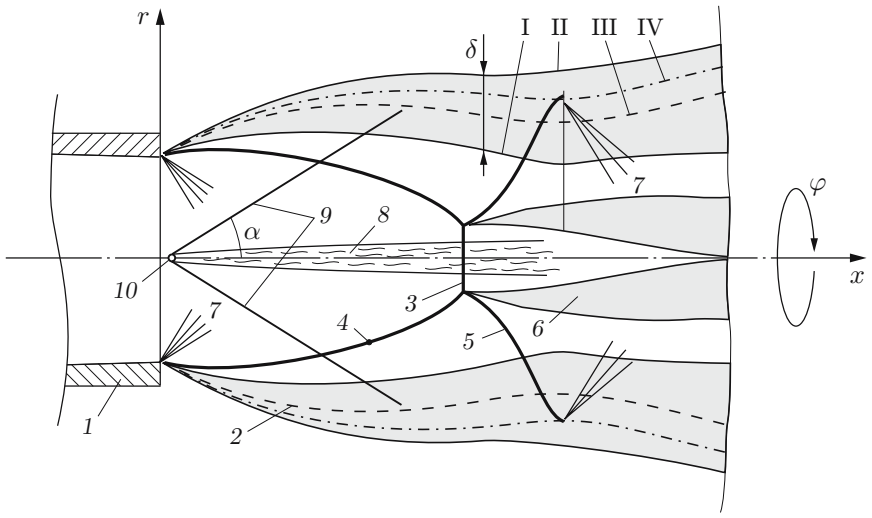

Fig. 3. Flow structure at the initial section of a supersonic underexpanded jet in the presence of a microjet: 1) nozzle ($R_a = 15$ mm); 2) shear layer (the inner and outer boundaries are indicated by I and II, respectively, the middle of the shear layer is indicated by III, and the line with a constant value M = 1 is indicated by IV); 3) Mach disk; 4) barrel shock wave; 5) reflected shock wave; 6) shear layer formed behind the point of intersection of the shock waves 3, 4, and 5; 7) expansion fan; 8) microjet wake; 9) Mach waves; 10) micronozzle.

location with respect to the main nozzle is defined by the parameters $\bar{x}_j = 0.167$ and $\bar{r}_j = 1.13$ ($\bar{x}_j = x_j/R_a$ is the distance between the main nozzle exit and the micronozzle center and $\bar{r}_j = r_j/R_a$ is the distance between the axis of symmetry of the main supersonic flow of the underexpanded jet and the micronozzle exit).

The main shock-wave elements in the pattern of interaction of a supersonic underexpanded jet with a microjet are schematically illustrated in Fig. 3.

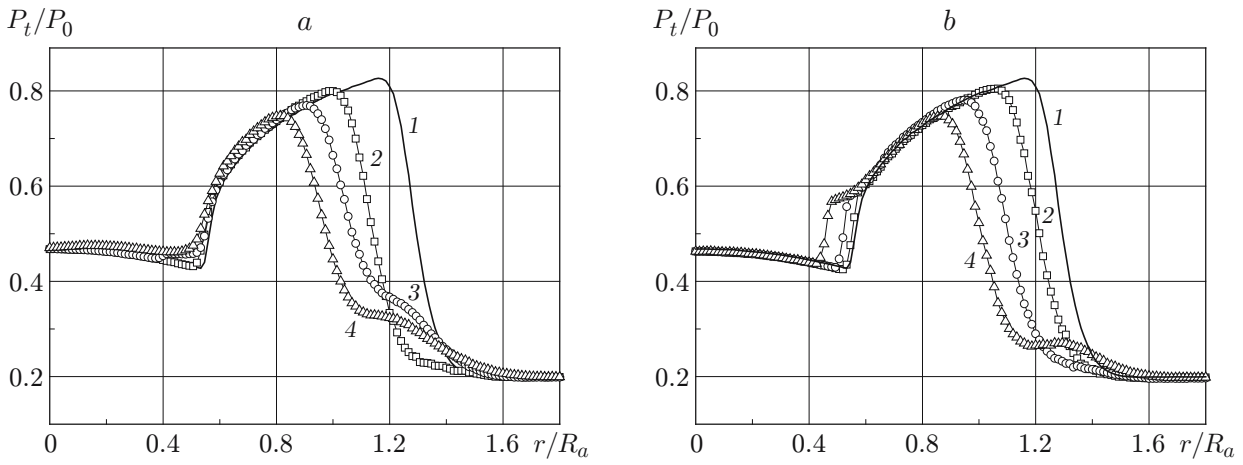

Fig. 4. Radial distributions of the relative Pitot pressure in the longitudinal section of the jet $x/R_a = 2$ with different locations of the micronozzle: (a) $\bar{x}_j = 0.167$ and $\bar{r}_j = 1.13$; (b) $\bar{x}_j = 0.67$ and $\bar{r}_j = 1.67$; the curves show the results for $N_j = 0$ ("clear jet") (1), 1.33 (2), 2.22 (3), and 4.44 (4).

TABLE 1

Location of the Shear Layer Boundaries at Different Gas-Dynamic Parameters

Jet type	r_1	r_2
"Clear" jet	1.16	1.5
$N_j = 1.33$	1.00	1.5
$N_j = 2.22$	0.90	1.6
$N_j = 4.44$	0.80	1.6

TABLE 2

Relative Thickness of the Shear Layer δ/R_a for Different Jets

	δ/R_a			
x/R_a	"Clear" jet	$N_j = 1.33$	$N_j = 2.22$	$N_j = 4.44$
1.5	0.22	0.38	0.52	0.72
2.0	0.40	0.58	0.70	0.87
3.0	0.44	0.69	0.90	0.99

The experiment was performed as follows. When a given pressure P_0 in the settling chamber of the jet module of the wind tunnel and the pressure P_{0j} in the settling chamber of the microjet device were reached and the location of the Pitot tube with respect to the streamwise axis x was fixed, the radial pressure profiles $P_t(r)$ were measured. After that, the values of the coordinates x and r were fixed, and the azimuthal pressure distribution $P_t(\varphi)$ was measured. The Pitot tube was moved with a step of 0.2 mm over the radius and with a step of 1° over the angle. The error of pressure measurement in the jet, which was equal to the root-mean-square deviation of pressure in time, reached 0.1%.

Typical radial profiles of the measured relative Pitot pressure for an undisturbed ("clear") jet and for a jet in the presence of microjets with different locations of the micronozzle are shown in Fig. 4. The pressure $P_t(r)$ was measured by a Pitot tube in one plane with the micronozzle axis at an angle $\varphi = 0°$ (see Fig. 1b). It follows from Fig. 4a that the inner boundary r_1 of the main jet corresponding to the maximum pressure on the profile is shifted toward the jet axis as the parameter N_j increases. The outer boundary of the jet r_2 for microjets with $N_j = 2.22$ and 4.44 corresponding to the radius $r/R_a = 1.6$ on the profile is also shifted. The microjet with $N_j = 1.33$ whose outer boundary almost coincides with the outer boundary for the "clear" jet and corresponds to the radius $r/R_a = 1.5$ (Table 1) exerts the smallest effect on the main flow. The data on the shear layer boundaries for different gas-dynamic parameters of microjets are summarized in Table 1.

Figure 4b shows the influence of the microjet intensity on the main jet structure. It is seen that the microjet effect on the main supersonic flow becomes more pronounced as the parameter N_j increases. In the range of radii $r/R_a = 0.45$–0.55, deformation of the barrel shock is observed. In the "clear" jet, the barrel shock is observed at a distance $r/R_a = 0.53$ from the jet axis. In the presence of a microjet with $N_j = 2.22$, the barrel shock occurs at $r/R_a = 0.51$, while the barrel shock location for a microjet with $N_j = 4.44$ corresponds to $r/R_a = 0.45$. For a microjet with $N_j = 1.33$, the location of the barrel shock wave coincides with its location in the case of a "clear" jet. For supersonic microjets with $N_j = 2.22$ and 4.44, an increase in the streamwise coordinate of the micronozzle x_j leads to stronger deformation of the barrel shock (bending toward the jet axis).

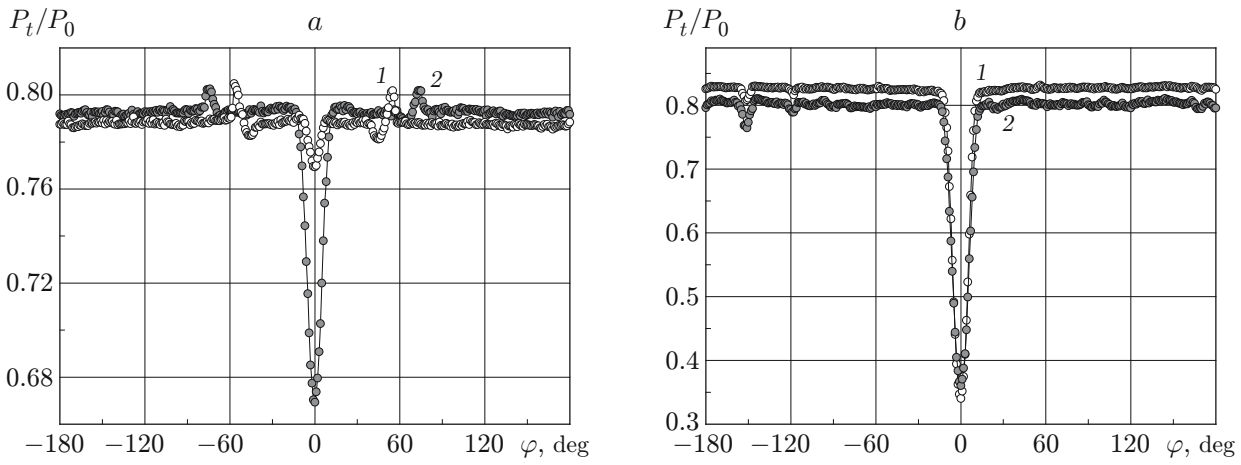

Fig. 5. Azimuthal distributions of the relative pressure in the presence of a microjet with the parameters $N_j = 2.22$, $\bar{x}_j = 0.167$, and $\bar{r}_j = 1.13$: (a) $r/R_a = 1.0$; (b) $r/R_a = 1.2$; curves 1 and 2 refer to $x/R_a = 1.5$ and 2.0, respectively.

The thickness of the shear layer of the jet $\delta/R_a = r_2 - r_1$ was determined in experiments in three longitudinal sections $x/R_a = 1.5$, 2.0, and 3.0 at $\varphi = 0°$ (Table 2). The thickness of the shear layer was found to increase with increasing microjet intensity; hence, the mixing process in the region of the microjet action is more intense. At constant microjet parameters ($N_j = 1.33$, 2.22, and 4.44, $\bar{x}_j = 0.167$, and $\bar{r}_j = 1.13$) and the values of the streamwise x and radial r coordinates of the main supersonic jet, the azimuthal pressure distributions $P_t(\varphi)$ were determined. Fifteen azimuthal distributions of the Pitot pressure measured by the Pitot tube were obtained for each section of the jet. The locations of the radial sections were varied in the range from $r/R_a = 0.8$ ($r = 12$ mm) to $r/R_a = 1.7$ ($r = 25$ mm). The azimuthal distributions of the relative pressure for the radial sections of the jet $r/R_a = 1.0$ and 1.2 with a constant gas-dynamic regime of the injected microjet flow ($N_j = 2.22$) in two longitudinal sections of the jet $x/R_a = 1.5$ and 2.0 are plotted in Fig. 5. At $\varphi = 0°$, the minimum of the measured Pitot pressure corresponds to the microjet axis and is caused by the wake formed behind the microjet interacting with the main jet flow and by the formation of two large-scale vortex structures induced by such interaction. The Taylor–Görtler instability is known to occur in the shear layer of a supersonic underexpanded jet. Pressure inhomogeneities registered in the azimuthal direction are caused by the presence of streamwise vortices of the Taylor–Görtler type in the shear layer of the underexpanded jet. The formation and development of these vortices are caused by the "negative curvature" of the streamlines [6].

The minimum value of pressure is $P_t/P_0 = 0.77$ in the section $x/R_a = 1.5$ (see Fig. 5a) and $P_t/P_0 = 0.67$ in the section $x/R_a = 2.0$. In addition to the wake, symmetric pressure peaks are observed, whose magnitude is rather small, as compared with the absolute value of the minimum pressure (at $\varphi = 0°$). It is seen in Fig. 5 that the maximum values of pressure are almost identical. The flow in this radial section corresponds to a supersonic flow in the region between the barrel shock and the inner boundary of the supersonic underexpanded jet.

In addition to disturbances induced by the main action of the microjet, there are also comparatively weak disturbances caused by the presence of a shock wave ahead of the microjet. At a distance from the nozzle exit $x/R_a = 1.5$ and 2.0, in the supersonic part of the jet, these disturbances become attenuated and can be considered as the Mach waves. Disturbances of the Mach wave type propagate at an angle α: $\sin\alpha = 1/\mathrm{M}$ (M is the local Mach number) [7]. The angle α can be determined from the relation $\tan\alpha = r\,\Delta\varphi/\Delta x$, where $\Delta\varphi$ is the difference in the angles φ_M at $x/R_a = 2.0$ and $x/R_a = 1.5$; φ_M is the value of the angle at which the pressure peaks corresponding to the Mach waves in Fig. 5a are registered ($\varphi_\mathrm{M} = 74°$ for $x/R_a = 2.0$ and $\varphi_\mathrm{M} = 54°$ for $x/R_a = 1.5$); $\Delta x = 7.5$ mm; the distance between the sections $x/R_a = 2.0$ and 1.5; $r = 15$ is the jet radius at which the Mach waves are registered. The calculated Mach angle is $\alpha = 33.5°$ and corresponds to the Mach number M = 1.81. This Mach number is close to the jet Mach number calculated by the formula for an isentropic flow $\mathrm{M}_j = \sqrt{2[(P_0/P_c)^{(\gamma-1)/\gamma} - 1]/(\gamma-1)}$, which was maintained constant and equal to $\mathrm{M}_j = 1.71$ in the experiment.

Figure 5b shows the azimuthal pressure profiles obtained in the shear layer of an underexpanded jet at $r/R_a = 1.2$, which corresponds to the middle of the shear layer of the main jet, where the maximum root-mean-

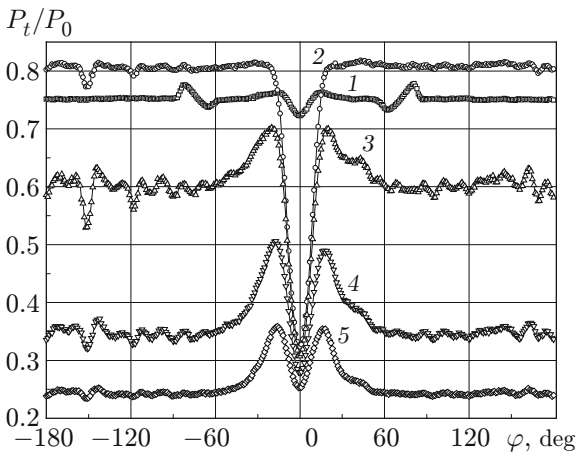

Fig. 6

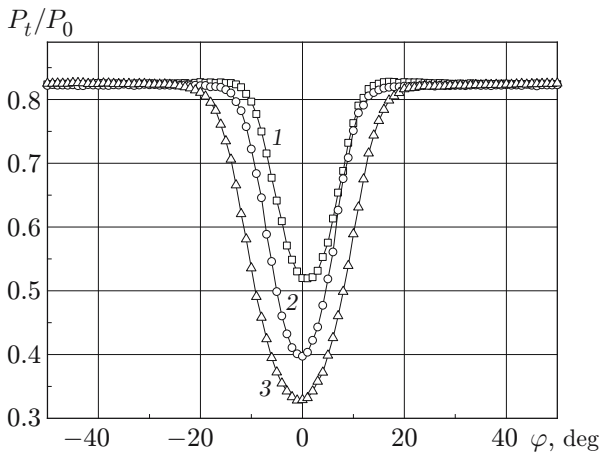

Fig. 7

Fig. 6. Azimuthal distributions of the relative pressure for a microjet with $N_j = 4.44$, $x/R_a = 2.0$, and $r/R_a = 0.87$ (1), 1.20 (2), 1.27 (3), 1.33 (4), and 1.40 (5).

Fig. 7. Azimuthal distributions of the relative pressure at $r/R_a = 1.13$ for microjets with $N_j = 1.33$ (1), 2.22 (2), and 4.44 (3).

square deviation of the measured Pitot pressure is observed [5]. The minimum values of pressure caused by the presence of the microjet differ insignificantly. Figure 5b shows a local minimum of pressure, which occurs at $\varphi = -151°$ and is caused by the presence of natural microroughness (scratches) on the inner surface of the nozzle.

Typical azimuthal distributions of pressure for different radial locations of the Pitot tube are shown in Fig. 6. It is seen that the data obtained for different values of the radius r are in good agreement. It is also seen in Fig. 6 that the dependences $P_t(\varphi)$ are similar because of the presence of the microjet. There are symmetric pressure peaks corresponding to the Mach waves in the region between the barrel shock and the inner boundary of the main jet (curve 1 in Fig. 6). As the radius increases, in addition to the minimum registered in the shear layer of the jet at $\varphi = 0°$, at $\varphi = \pm 20°$, $r/R_a = 1.27$, and at $\varphi = \pm 17°$, $r/R_a = 1.33$ and 1.40, there arise additional pressure maximums (curves 3–5 in Fig. 6). The absolute minimum and maximum deviations of pressure become commensurable on the outer boundary of the jet ($r/R_a = 1.4$) (curve 5 in Fig. 6). The emergence of the maximums located symmetrically with respect to the pressure minimum at $\varphi = 0°$ is caused by the formation of two streamwise vortices. The formation of two large-scale counter-rotating streamwise vortices generates a radial flow (pressure minimum at $\varphi = 0°$) favoring the inflow of the low-pressure gas inward the jet. The pressure maximum arising at $\varphi = \pm(17–20)°$ corresponds to the high-pressure gas flow directed toward the outer boundary of the jet. The calculated scheme of such a flow formed behind a tab placed on the nozzle exit was given in [8]. At $\varphi = 0°$, the minimum value of pressure increases in proportion to the increase in intensity of the injected microjet (Fig. 7).

To conclude, we should note that two longitudinal vortex structures are formed in the shear layer because of interaction of the main jet with a microjet located close to the nozzle axis if the microjet axis is perpendicular to the main jet axis. The shock wave formed ahead of the microjet in the main jet flow penetrates deep inward this jet and induces flow disturbances in the region between the barrel shock and the inner jet boundary and deformation of the barrel shock wave. The most pronounced effect is exerted by the microjet with the maximum pressure (microjet with $N_j = 4.44$). As the pressure in the microjet increases, local deformation of the shear layer of the main underexpanded jet occurs, which can be treated as an increase in the shear layer thickness.

Disturbances of two types are observed in the interaction of the microjet with the main jet. The stronger disturbance is caused by the presence of the wake component of the microjet and by generation of two streamwise vortices. The weaker disturbance is manifested in the form of the Mach-wave-type disturbances propagating in the supersonic region of the shear layer of the main jet. The intensity of the microjet wake increases with increasing total pressure in the microjet. Absolute controllability of the geometric and gas-dynamic parameters of the microjet and the resultant stationary disturbance in the jet flow region in experiments with microjets should be noted.

This work was supported by the Russian Foundation for Basic Research (Grant No. 05-08-01215).

REFERENCES

1. E. Collin, S. Barre, and J. P. Bonnet, "Supersonic mixing enhancement by radial fluid injection," in: *Proc. of the EUROMECH Colloquium 403* (Poitiers, France, November 2–4, 1999), Futuroscope, Poitiers (2000), pp. 55–64.
2. M. B. Alkislar, A. Krothapalli, I. Choutapalli, and L. Lourenco, "Structure of supersonic twin jets," *AIAA J.*, **43**, No. 11, 2309–2318 (2005).
3. Huadong Lou, Farrukh S. Alvi, and Chang Shih, "Active and passive control of supersonic impinging jets," *AIAA J.*, **44**, No. 1, 58–66 (2006).
4. K. M. Khritov, V. Ye. Kozlov, S. Yu. Krasheninnikov, et al., "On the prediction of turbulent jet noise using traditional aeroacoustic methods," *Int. J. Aeroacoustics*, **4**, Nos. 3/4, 289–324 (2005).
5. V. I. Zapryagaev, N. P. Kiselev, and A. A. Pavlov, "Effect of streamline curvature on intensity of streamwise vortices in the mixing layer of supersonic jets," *J. Appl. Mech. Tech. Phys.*, **45**, No. 3, 335–434 (2004).
6. V. I. Zapryagaev and A. V. Solotchin, "Three-dimensional structure of flow in a supersonic underexpanded jet," *J. Appl. Mech. Tech. Phys.*, **32**, No. 4, 503–507 (1991).
7. N. E. Kochin, I. A. Kibel, and N. V. Rose, *Theoretical Hydrodynamics* [in Russian], Part 2, Fizmatgiz, Moscow (1963).
8. V. I. Zapryagaev, I. N. Kavun, N. P. Kiselev, and A. V. Solotchin, "Effect of large-scale streamwise vortices on the flow in a supersonic underexpanded jet," in: *Jet, Separated, and Unsteady Flows*, Abstr. of 21st All-Russia Workshop (Novosibirsk, August 15–18, 2007), Parallel, Novosibirsk (2007), pp. 112–113.